UDC 621.867.8:681.586

Vitaliy Korendiy¹, Oleksandr Yaniy², Taras Vilchynskyi³, Volodymyr Piharev⁴

¹ Lviv Polytechnic National University, ORCID: 0000-0002-6025-3013,

e-mail: vitalii.m.korendii@lpnu.ua

² Lviv Polytechnic National University, ORCID: 0009-0001-2491-5278,

e-mail: oleksandr.m.yaniv@lpnu.ua

³ Lviv Polytechnic National University, ORCID: 0009-0001-1247-7960,

e-mail: taras.r.vilchynskyi@lpnu.ua

⁴ Lviv Polytechnic National University, ORCID: 0009-0005-8532-2483,

e-mail: volodymyr.pigarev.mmprs.2024@lpnu.ua

KINETOSTATIC ANALYSIS OF THE PROPULSION SYSTEM FOR A MOBILE IN-PIPE INSPECTION ROBOT

https://doi.org/10.23939/istcipa2023.59.010

Ó Korendiy V., Yaniv O., Vilchynskyi T., Piharev V., 2025

Problem statement. The structural integrity of extensive pipeline networks is critical for economic and environmental safety, demanding reliable inspection methods. Mobile In-Pipe Inspection Robots (IPIRs) offer a nondisruptive solution; however, the design of their propulsion systems for confined and complex environments remains challenging. Existing analytical frameworks often exhibit a disconnect between kinematic modeling (motion planning) and force analysis (stability and traction), particularly for advanced hybrid locomotion strategies. This gap hinders the systematic optimization and control of IPIR designs. Purpose. This research aims to develop and analyze a comprehensive kinetostatic model for the propulsion system of a specific IPIR design: a two-module robot utilizing an inchworm locomotion strategy, driven by an internal slider-crank mechanism and rectified by overrunning clutches. The goal is to establish a mathematical model that accurately links the kinematics of motion with the forces required to execute it. Methodology. The study employs a kinetostatic analysis based on the Lagrangian approach. The robot is conceptualized as a hybrid dynamic system operating in two distinct modes: expansion and contraction. The crank rotation angle is adopted as the generalized coordinate. Equations of motion are derived for each mode, accounting for the constraints imposed by the ideal overrunning clutches, which enforce unidirectional movement. The resulting stiff and non-smooth differential equations are implemented in Wolfram Mathematica and solved numerically using the "StiffnessSwitching" method to handle the discontinuous dynamics accurately. Results. The numerical simulation successfully validates the inchworm locomotion principle, demonstrating the characteristic alternating movement of the modules. Under a constant driving torque (0.25 N·m), the robot exhibits continuous acceleration, with peak velocities approaching 4 m/s within the first second. Analysis of the velocity profiles confirms the non-overlapping nature of the module movements, validating the idealized clutch model. A key finding is the presence of extremely large acceleration spikes occurring instantaneously at the transitions between expansion and contraction modes, highlighting significant dynamic impacts inherent in this locomotion strategy. Novelty. The novelty lies in the rigorous derivation of a kinetostatic framework specifically tailored to an inchworm IPIR with overrunning clutches. By applying Lagrangian mechanics to this hybrid dynamic system, the study provides a unified analytical foundation that bridges the gap between motion generation and force analysis for this class of robots. Practical value. The developed mathematical model serves as a powerful tool for optimizing the design parameters (e. g., mass distribution, linkage geometry, actuator sizing) of inchworm IPIRs. It provides critical insights into the system's dynamic behavior, particularly emphasizing the need to mitigate the high dynamic loads generated during clutch engagement in practical implementations. Scope of further investigations. Future research should focus on refining the model to incorporate nonideal clutch behaviors (e.g., compliance and friction dynamics), analyzing locomotion in complex geometries (bends and vertical sections), and developing model-based control strategies.

Keywords: in-pipe inspection robot, kinetostatic analysis, inchworm locomotion, hybrid dynamic system, Lagrangian mechanics, overrunning clutch, slider-crank mechanism, mathematical modeling, numerical simulation.

Introduction. Problem Statement

Pipelines are a critical infrastructure for transporting essential resources such as oil, gas, and water over vast distances. The structural integrity and operational safety of these networks are paramount, necessitating regular inspection and maintenance to prevent failures that could lead to significant economic losses and severe environmental damage. Traditional inspection methods are often costly, time-consuming, and may require a complete shutdown of the system.

In recent years, mobile in-pipe inspection robots have emerged as a highly effective solution to these challenges. These robotic systems can navigate complex pipeline networks to perform diagnostic tasks like corrosion detection, weld inspection, and leak identification without significant disruption to operations. The performance of such a robot is critically dependent on its propulsion system, which must ensure stable locomotion, provide sufficient traction, and overcome obstacles such as bends, welds, and changes in pipe diameter.

To design an efficient and reliable propulsion system, a deep understanding of the interplay between the mechanism's kinematics and the forces involved is essential. Kinetostatic analysis, which combines the study of motion and forces, provides a powerful framework for modeling and optimizing these complex electromechanical systems. This paper presents a comprehensive kinetostatic analysis of a propulsion system for a mobile in-pipe inspection robot. The primary objective is to develop a mathematical model that accurately describes the relationship between actuator inputs, contact forces, and the robot's motion, thereby providing a robust analytical foundation for future design and optimization.

The effective design of a propulsion system for an in-pipe robot presents a significant engineering challenge. The core problem lies in achieving stable and reliable locomotion within a confined and often unpredictable environment. An improperly designed system may suffer from issues such as wheel slippage, insufficient traction to climb vertical sections, jamming at obstacles, or excessive power consumption. Therefore, this research aims to address the fundamental problem of lacking a comprehensive analytical framework for these systems. This study seeks to develop a robust kinetostatic model enabling a more systematic and efficient approach to the design of in-pipe inspection robots.

Literature Review

Pipelines constitute the arterial infrastructure of modern industrial society, serving as the primary conduits for the transport of critical resources such as water, natural gas, and oil [1]. The structural integrity of these vast networks is paramount; however, they are subject to continuous degradation over time. Environmental factors and operational stressors lead to deterioration in the form of corrosion, cracking, strain aging, and creep deformation, which can compromise the pipeline's structural safety [2]. The consequences of failure are severe, ranging from significant financial losses for operators to catastrophic environmental contamination and risks to human safety [1]. This reality necessitates a robust and reliable regime of periodic inspection and maintenance to ensure the continued safe and cost-effective operation of this essential infrastructure [2].

The physical nature of pipeline networks presents formidable challenges to inspection. Many pipelines are buried underground, span vast distances, and feature complex geometries with numerous bends and branches, making direct human access difficult, hazardous, and often impossible [3]. Traditional inspection methods that require excavation are disruptive and prohibitively expensive, especially in urban environments [3]. Consequently, the field has increasingly turned to robotic solutions to overcome these limitations. Mobile In-Pipe Inspection Robots (IPIRs) have emerged as the most economical and effective technology for performing internal pipeline assessments without requiring destructive or disruptive access [1]. These robotic platforms serve as mobile sensor carriers, deploying a suite of Non-Destructive Testing tools – including high-resolution cameras, ultrasonic transducers, and magnetic flux leakage sensors – to gather high-fidelity data on the internal condition of the pipe wall [2].

The development of IPIRs is not a purely academic endeavor but is fundamentally driven by a strong "technology pull" from industry. The immense economic and environmental stakes associated with pipeline failure create a powerful and persistent demand for more capable and autonomous robotic systems. This demand has spurred a remarkable diversification in robot design, with researchers proposing a wide array of locomotion strategies to tackle the varied and challenging conditions found within pipelines, such as changes in diameter, vertical sections, sharp bends, and the presence of obstacles or debris [2]. The evolution from simple wheeled crawlers to complex, multi-module, bio-inspired machines is a direct engineering response to the escalating industrial requirements for greater operational reliability, safety, and versatility.

While a multitude of IPIR designs have been conceptualized and prototyped, the performance of these robots is fundamentally governed by the efficacy of their propulsion systems. The ability to generate sufficient traction, adapt to changing pipe geometry, and maintain stability is critical for successful inspection missions. A deep understanding of the interplay between the forces generated by the robot's actuators and the resulting motion is therefore essential for robust design and intelligent control. However, the analytical models used to describe this interplay often fall into one of two categories: simplified static or kinematic models that neglect crucial dynamic effects, or highly complex dynamic simulations tailored to unconventional locomotion principles.

Wheeled and tracked robots represent the most straightforward approach to in-pipe locomotion, relying on the principle of rolling contact to generate motion. These systems are often favored for their mechanical simplicity, high potential mobility, and lower frictional losses compared to sliding mechanisms [1]. The simplest configuration is the standard wheeled robot, which functions much like a terrestrial mobile robot but constrained within a cylindrical workspace. These designs are effective in horizontal or slightly inclined pipes but are fundamentally limited by traction; they typically lack the ability to climb vertical sections due to insufficient normal force to counteract gravity, leading to slippage. To overcome this limitation in ferromagnetic pipelines, some designs incorporate magnetic wheels, which generate an adhesive force that enables vertical climbing [1].

Tracked systems, also known as caterpillar-type robots, replace wheels with continuous tracks. This design significantly increases the contact area with the pipe wall, which in turn enhances traction and stability, making these robots better suited for navigating uneven surfaces or pipes with debris [4]. The larger contact patch provides a more robust grip, reducing the likelihood of slippage compared to wheeled counterparts [5]. However, both standard wheeled and tracked systems, in their basic forms, struggle with significant variations in pipe diameter and require additional mechanisms to adapt.

The wall-press architecture is arguably the most prevalent and versatile design paradigm in the field of IPIRs [6]. The core principle of a wall-press system is the active generation of a normal force against the inner pipe wall. This pressing force, which is independent of gravity, ensures sufficient friction for the driving wheels or tracks to generate traction. This capability is what enables wall-press robots to reliably climb vertical pipes, navigate inverted sections, and maintain stability across a range of orientations [1].

The prevalence of this design philosophy has led to a clear evolutionary trend away from simple, single-locomotion systems toward more complex hybrid architectures. The limitations of basic wheeled robots, such as their inability to climb vertically, directly spurred the innovation of hybrid systems that integrate a wall-press mechanism. Consequently, the most common and capable IPIRs are often described as "wheeled wall-press" or "caterpillar wall-press" types [1]. This fusion of concepts, combining the mobility of wheels or tracks with the traction-generating capability of a wall-press mechanism, represents a significant advancement. It underscores a design trend where the most versatile robots are modular systems that combine the strengths of multiple approaches to overcome the weaknesses of any single one [7]. This move towards hybridization indicates that the frontier of IPIR research lies in understanding and optimizing these more complex, integrated systems.

Screw-drive robots employ a unique locomotion principle based on helical motion. These robots are equipped with wheels that are inclined at a fixed angle relative to the robot's longitudinal axis [1]. When the wheels are rotated by a central motor, their angled orientation causes the entire robot to move like a screw, simultaneously translating along the pipe axis and rotating about it [2].

This mechanism offers several distinct advantages. It can generate substantial propulsive force, providing good power characteristics, and its streamlined profile often results in less obstruction to fluid flow within the pipe compared to bulky wall-press systems [2]. However, this design also comes with significant drawbacks. The helical motion is inherently slow, and the mechanical complexity required for steering is considerable [1]. Furthermore, reversing the robot's direction of travel is often a difficult operation [2]. Notable examples in the literature that explore this concept include the work of Nishimura et al., who designed a two-segment robot connected by a universal joint for enhanced flexibility [2], and Kakogawa et al., who developed a screw-type robot aimed at solving challenges related to navigating bends and branches [5].

Drawing inspiration from biology, another class of IPIRs utilizes inchworm-like or peristaltic locomotion [3]. These robots typically consist of at least two clamping modules and an extending/contracting actuator. The motion cycle involves anchoring one module to the pipe wall, extending or contracting the central body, anchoring the second module, and then releasing the first. By repeating this sequence, the robot "inches" its way through the pipe [5].

A key challenge for inchworm robots is generating sufficient traction, particularly in low-friction environments. To address this, many designs incorporate self-locking mechanisms, such as wedges or anisotropic fins, which engage with the pipe wall to prevent backward slippage during the extension phase [5]. While this locomotion method can be effective in navigating highly constrained or irregular environments, it is inherently intermittent and generally slower than wheeled or tracked motion [3]. The emerging field of soft robotics has found a natural application in this category, with researchers developing worm-like robots from soft, compliant materials that can readily conform to their environment [8]. This category also encompasses other bio-inspired designs, such as snake-like (serpentine) robots, which use undulatory motion to propel themselves, and legged (walking) robots, which offer high mobility over obstacles but are mechanically complex, requiring multiple actuators and sophisticated control systems [2].

Pipe Inspection Gauges, or PIGs, represent a class of passive robots that lack an onboard propulsion system [7]. Instead, they are propelled through a pipeline by the differential pressure of the fluid (liquid or gas) flowing within it [2]. A PIG is inserted into the pipe via a launcher and is carried along with the product flow until it is captured at a receiving station [6]. Their primary advantage is that they require no power for locomotion, making them suitable for very long-distance inspections [7].

However, this passivity is also their greatest limitation. The motion of a PIG is entirely dependent on the fluid flow and cannot be controlled; its velocity can fluctuate unpredictably, and it cannot be stopped or reversed [5]. PIGs are notoriously poor at navigating complex pipe geometries, often getting stuck at sharp bends, T-junctions, or sudden changes in pipe diameter [1]. While they serve an important role in routine pipeline maintenance, their lack of maneuverability and control makes them unsuitable for detailed inspection tasks that require precise positioning or navigation through complex networks.

The diverse array of propulsion mechanisms developed for IPIRs reflects the complexity of the inpipe environment. Each design represents a unique set of trade-offs between speed, traction, adaptability, and mechanical complexity. The transition from conceptual design to a functional and reliable IPIR necessitates the use of rigorous analytical frameworks to predict and optimize performance. The literature on IPIRs employs a range of modeling techniques, primarily falling into the categories of kinematics, statics, and dynamics. These models are essential for tasks such as motion planning, ensuring stability, and sizing actuators. However, a critical examination of these frameworks reveals a significant disconnect between the analysis of motion and the analysis of the forces required to produce that motion, a gap that motivates the exploration of kinetostatic modeling.

Kinematic analysis is concerned with the geometry of motion, describing the position, velocity, and acceleration of a robot's components without consideration of the forces and torques that cause the motion [9]. For IPIRs, the primary objective of kinematic modeling is to understand and control the robot's pose (position and orientation) within the constrained three-dimensional cylindrical workspace of the pipe [10]. This is crucial for planning trajectories through complex geometries like elbows and T-junctions and for determining the actuator commands needed to execute those trajectories [9].

To ensure that a robot can execute the motions prescribed by its kinematic model, an analysis of the forces involved is essential. This analysis is critical for guaranteeing stability, preventing slip, and appropriately sizing actuators and structural components. Numerous literatures, particularly [11]–[15], present a spectrum of approaches, from simplified static analyses to more comprehensive dynamic simulations. A critical component in both static and dynamic models is the treatment of friction. While many analyses rely on a simplified constant coefficient of friction, the reality of the wheel-pipe interaction can be far more complex. Research in related fields, such as concentric tube robotics, has shown that friction can be a highly non-linear and configuration-dependent phenomenon, arising from both distributed contact forces and concentrated moments at points of geometric discontinuity [16]. Neglecting these complexities can lead to significant errors in predicting robot behavior, particularly in systems with intricate contact mechanics. For IPIRs, especially those operating in potentially wet or contaminated pipes, an oversimplified friction model can lead to an underestimation of required actuator torques and an increased risk of slip.

The current state of the literature reveals a clear analytical disconnect. Kinematic models are developed to plan desired motion profiles, assuming perfect traction. Separately, static models are developed to determine the minimum conditions for stability under simplified assumptions. There is a missing link that addresses the crucial question: for a given desired velocity and acceleration profile of the robot body, what are the precise, time-varying forces and torques that must be generated by the actuators and transmitted through the complex, multi-contact propulsion mechanism to execute that motion? For example, as a robot enters a curve, the normal and tractive forces required at each wheel will change dynamically to provide the necessary centripetal acceleration and to counteract varying slip tendencies. A simple passive spring system may be unable to provide these varying forces optimally, and a controller without a model of this relationship cannot command an active system effectively. This gap highlights a compelling need for a kinetostatic framework that directly links the kinematics of motion with the statics of force transmission, providing a sophisticated tool for model-based control and design optimization that is currently lacking in the field.

Main Objectives and Tasks of Research

A comprehensive review of the literature on in-pipe inspection robots reveals a field that has matured significantly, evolving from simple crawlers to complex, multi-functional robotic systems. This evolution has been driven by persistent industrial demands for robots capable of navigating increasingly challenging pipeline environments. The design paradigm has clearly shifted towards hybrid, modular systems, most commonly wheeled or tracked platforms that utilize active wall-pressing mechanisms to ensure traction and adaptability. This trend towards mechanical complexity, however, has outpaced the development of corresponding analytical frameworks for design and control. A synthesis of the literature exposes a critical gap between the methods used to model robot motion and the methods used to analyze the forces required to create that motion. This identified gap points directly to the need for a kinetostatic model for the propulsion systems of advanced IPIRs.

Kinetostatics directly relates the kinematics of motion (desired velocities and accelerations) to the statics of force transmission, providing a unified framework that is currently missing. It answers the critical question of what actuator efforts are required to achieve a specific motion state. By leveraging the quasi-static assumption valid for many inspection scenarios, a kinetostatic model offers a powerful analytical tool that is less computationally intensive than full dynamic simulation, making it suitable for both offline design optimization and online, model-based control. A robust kinetostatic model would enable engineers to more accurately size actuators, optimize linkage geometries for force transmission, and develop sophisticated control algorithms that can actively manage traction and stability during complex maneuvers.

The development of a comprehensive kinetostatic model for the propulsion system of a mobile in-pipe inspection robot addresses a well-defined and significant deficiency in the existing body of scientific literature. It promises to apply a higher level of analytical rigor, inspired by the deep dynamics paradigm, to the mainstream and industrially relevant class of complex, hybrid IPIRs. This endeavor is poised to advance the design, control, and ultimate performance of the next generation of robotic systems for pipeline integrity management.

System Description and Assumptions

This research extends the authors' previous investigations presented in [17]–[20] and is focused on the kinetostatic analysis of a propulsion system of an in-pipe robot shown in Fig. 1. The robot consists of two modules with masses m_1 and m_2 . They are connected by a slider-crank mechanism: a crank AB (length r) rotating about point A within module m_1 , and a connecting rod BC (length L) joined to module m_2 at point C. The wheels are equipped with overrunning clutches, which prevent backward motion and enforce unidirectional locomotion along the Ox-axis.

Let us establish the following assumptions for the simplified mathematical model: 1) 1D motion: The robot moves along a straight, horizontal pipeline. Motion is restricted to the Ox-axis; 2) coordinate system: x_1 and x_2 denote the positions of points A and C, respectively, in the considered inertial reference frame Oxy. The generalized coordinate φ is the angle of the crank AB measured from the horizontal axis, as depicted in the diagram (Fig. 1); 3) simplified kinematics: let us assume the connecting rod length is significantly larger than the crank radius $(L \gg r)$. This allows for a first-order approximation of the kinematics; 4) inertia and forces: the rotating components (crank and motor rotor) have a combined moment of inertia J_A about point A. A driving torque M is applied to the crank. During forward motion, the modules experience rolling resistance (friction) forces F_{r1} and F_{r2} ; 5) ideal clutches: the clutches perfectly prevent backward motion: $\dot{x}_1 \ge 0$ and $\dot{x}_2 \ge 0$.

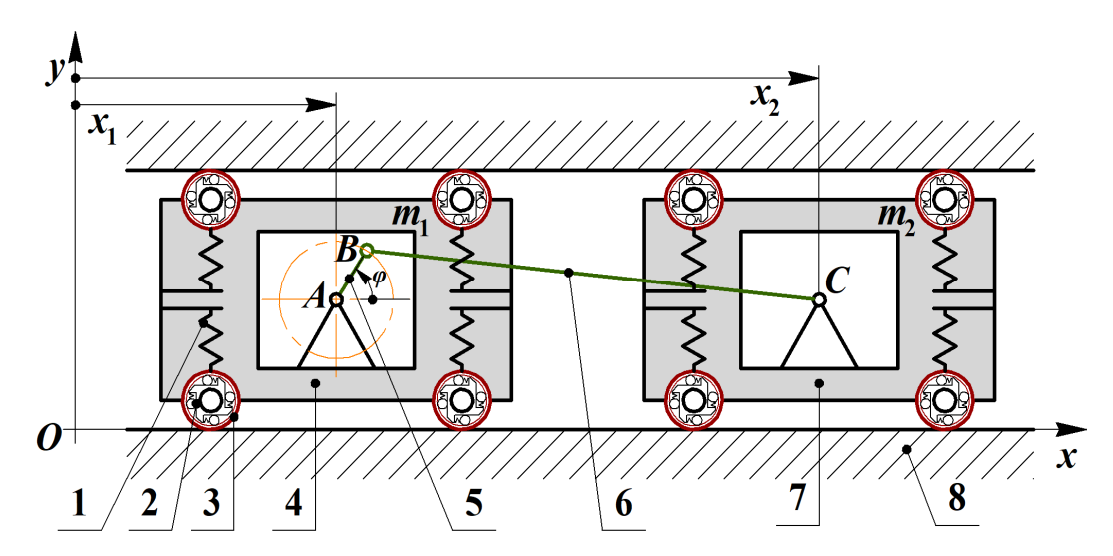


Fig. 1. Simplified kinematic diagram of the propulsion system of a mobile in-pipe robot: 1 – wheel pressure spring; 2 – overrunning clutch (freewheel clutch); 3 – wheel; 4, 7 – rear and front mobile modules; 5 – driving crank; 6 – connecting rod; 8 – pipe wall

Рис. 1. Спрощена кінематична схема привідного механізму мобільного робота: 1—притискна пружина колеса; 2—обгінна муфта (муфта вільного ходу); 3— колесо; 4, 7— задній і передній рухомі модулі; 5— привідний кривошип; 6— шатун; 8— стінка трубопроводу

Kinematic Analysis

The following analysis presents a thorough derivation of the equations of motion for the in-pipe robot shown in the kinematic diagram (Fig. 1). The derivation employs the Lagrangian approach for the kinetostatic analysis and adopts the crank rotation angle φ as the generalized coordinate.

Let us first determine the relationship between the generalized coordinate φ and the positions x_1 , x_2 . The distance between the modules is $S = x_2 - x_1$.

Based on the definition of φ (measured from the Ox-axis), the horizontal position of B relative to A is $r \cdot \cos(\varphi)$. Under the assumption $L \gg r$, the connecting rod BC remains nearly horizontal, and its horizontal projection is approximately L. The distance S is approximated as:

$$S(j) \gg L + r \times cos(j)$$
. (1)

The relative velocity between the modules is $\dot{S} = \dot{x}_2 - \dot{x}_1$ and, based on (1), equals to:

$$\mathcal{S} = \frac{dS}{d\mathbf{j}} \dot{\mathbf{j}} \mathbf{k} \tag{2}$$

Let us define the kinematic transfer function $K(\varphi)$:

$$K(\mathbf{j}) = \frac{dS}{d\mathbf{j}} = -r \times \sin(\mathbf{j}). \tag{3}$$

Thus, the relative velocity is:

$$\mathcal{S}(j,j\&) = K(j) \times j\& \tag{4}$$

We also require the derivative of $K(\varphi)$ with respect to φ for the dynamic analysis:

$$K \not (j) = \frac{dK}{di} = -r \times \cos(j). \tag{5}$$

Locomotion Principle and Modes

The robot utilizes an inchworm locomotion strategy. The internal actuation changes the distance *S*. The clutches rectify this internal oscillation into net forward movement by selectively locking one module. This leads to two distinct modes of operation.

Mode 1: Contraction $(\dot{S} < 0)$. The mechanism pulls the modules together. Module m_2 attempts to move backward and is locked by its clutch. Module m_1 moves forward. Condition: $K(j) \times \& < 0$. Constraint: $\dot{x}_2 = 0$. Velocity: $\& = -\& = -K(j) \times \&$.

Mode 2: Expansion $(\dot{S} > 0)$. The mechanism pushes the modules apart. Module m_1 attempts to move backward and is locked by its clutch. Module m_2 moves forward. Condition: $K(j) \not\ni \& > 0$. Constraint: $\dot{x}_1 = 0$. Velocity: $\& = \& = K(j) \not\ni \&$.

In both modes, the constraints imposed by the clutches reduce the system to a single degree of freedom, governed by φ .

Kinetostatic Analysis (Lagrange's Equations)

Let us use Lagrange's equations of the second kind to derive the equations of motion for each operation mode:

$$\frac{d}{dt} \mathop{\operatorname{geq}}_{\mathbf{I}} \frac{\ddot{\mathbf{G}}}{\mathbf{g}} \frac{\ddot{\mathbf{G}}}{\mathbf{g}} - \frac{\mathbf{I}}{\mathbf{I}} = Q_{\mathbf{j}} , \qquad (6)$$

where T is the total kinetic energy and Q_{φ} is the generalized force.

The total kinetic energy is:

$$T = \frac{1}{2} \times m_1 \times \mathcal{R} + \frac{1}{2} \times m_2 \times \mathcal{R} + \frac{1}{2} \times J_A \dot{\mathcal{S}} . \tag{7}$$

Mode 1: Contraction ($\dot{S} < 0$). Kinetic energy T_1 can be derived as follows, taking into account the corresponding constraints $(x_2 = 0, x_3 = -K(j))$:

$$T_{1} = \frac{1}{2} \times m_{1} \times \left(-K(j) \times j \mathcal{R}\right)^{2} + \frac{1}{2} \times J_{A} \times j \mathcal{R} = \frac{1}{2} \times \left(J_{A} + m_{1} \times \left(K(j)\right)^{2}\right) \times j \mathcal{R}. \tag{8}$$

Let us determine the generalized force $Q_{\varphi 1}$ using the principle of virtual work. Module m_1 moves forward, so the external force is $-F_{r1}$. The virtual work done by all the forces and moments is the following:

$$dW_1 = M \times dj + (-F_{r1}) \times dx_1. \tag{9}$$

The virtual displacements respect the constraints: $dx_2 = 0$, $dx_1 = -K(j) \times dj$. Therefore:

$$Q_{j} = M + F_{r1} \times K(j).$$
 (10)

Applying the Lagrange equation (6) and considering the effective moment of inertia $J_{eff.1} = J_A + m_1 \times (K(j))^2$, the equation of the robot locomotion during Mode 1 is the following:

$$J_{eff.1} \times \frac{dJ_{eff.1}}{di} \times \frac{dJ_{eff.1}}{di} \times \frac{dJ_{eff.1}}{di} = Q_{i1}, \tag{11}$$

where $\frac{1}{2} \times \frac{dJ_{eff.1}}{d\mathbf{j}} = m_1 \times K(\mathbf{j}) \times K(\mathbf{j})$.

Let us rewrite equation (11) in the following form:

$$\left(J_{A} + m_{1} \times \left(K\left(\mathbf{j}\right)\right)^{2}\right) \times \mathbf{j} \otimes + m_{1} \times K\left(\mathbf{j}\right) \times K\left(\mathbf{j}\right) \times K\left(\mathbf{j}\right) \times K\left(\mathbf{j}\right). \tag{12}$$

Substituting the approximations (3) and (5) into (12), we obtain:

$$(J_A + m_1 \times r^2 \times \sin^2(j)) \times \mathcal{M} + m_1 \times r^2 \times \sin(j) \times \cos(j) \times \mathcal{M} = M - F_{r_1} \times r \times \sin(j). \tag{13}$$

Mode 2: Expansion $(\dot{S} > 0)$. Kinetic energy T_2 can be derived as follows, taking into account the corresponding constraints $(\mathcal{K} = 0, \mathcal{K} = \mathcal{K} = K(j))$:

$$T_{2} = \frac{1}{2} \times m_{2} \times \left(K\left(\mathbf{j}\right) \times \mathbf{j} \right)^{2} + \frac{1}{2} \times J_{A} \times \mathbf{j} \right)^{2} = \frac{1}{2} \times \left(J_{A} + m_{2} \times \left(K\left(\mathbf{j}\right)\right)^{2}\right) \times \mathbf{j} \right)^{2}. \tag{14}$$

Let us determine the generalized force $Q_{\varphi 2}$ using the principle of virtual work. Module m_2 moves forward, so the external force is $-F_{r2}$. The virtual work done by all the forces and moments is the following:

$$dW_2 = M \times d\mathbf{j} + (-F_{r2}) \times dx_2. \tag{15}$$

The virtual displacements respect the constraints: $dx_1 = 0$, $dx_2 = K(j) \times dj$. Therefore:

$$Q_{j} = M - F_{r2} \times K(j)$$
. (16)

Applying the Lagrange equation (6) and considering the effective moment of inertia $J_{eff.2} = J_A + m_2 \times (K(j))^2$, the equation of the robot locomotion during Mode 2 is the following:

$$J_{eff.2} \dot{\gamma} \& + \frac{1}{2} \times \frac{dJ_{eff.2}}{d\dot{j}} \dot{\gamma} \& = Q_{j.2}, \tag{17}$$

where $\frac{1}{2} \times \frac{dJ_{eff,2}}{dj} = m_2 \times K(j) \times K(j)$.

Let us rewrite equation (17) in the following form:

$$\left(J_{A} + m_{2} \times \left(K(\mathbf{j})\right)^{2}\right) \times \mathcal{K} + m_{2} \times K(\mathbf{j}) \times K(\mathbf{j}) \times K(\mathbf{j}) \times \mathcal{K} = M - F_{r2} \times K(\mathbf{j}). \tag{18}$$

Substituting the approximations (3) and (5) into (18), we obtain:

$$(J_A + m_2 \times r^2 \times \sin^2(j)) \times \mathbf{k} + m_2 \times r^2 \times \sin(j) \times \cos(j) \times \mathbf{k}^2 = M + F_{r2} \times r \times \sin(j).$$
 (19)

Simplified Mathematical Model

The mathematical model of the in-pipe robot is a hybrid dynamic system, where the equations of motion switch depending on the sign of the relative velocity $\Re K(j)$ $\Im K = -r \times \sin(j)$

The model, using the generalized coordinate φ and the approximation $L \gg r$, is summarized as:

$$J_{eff.}(j) \dot{j} \otimes + C_{eff.}(j, j \otimes) = Q_{total}(j), \tag{20}$$

where the effective inertia $(J_{eff.})$, the centrifugal terms $(C_{eff.})$, and the generalized forces (Q_{total}) are defined piecewise:

1. Contraction phase (if $\Re -r \times \sin(j) \times \Re < 0$):

$$J_{eff.}(j) = J_A + m_1 \times x^2 \times \sin^2(j);$$

$$C_{eff.}(j, j \otimes) = m_1 \times x^2 \times \sin(j) \times \cos(j) \times \otimes ;$$

$$Q_{total}(j) = M - F_{rl} \times x \times \sin(j);$$
(21)

2. Expansion phase (if $\$ = -r \times \sin(j) \times \$ > 0$):

$$J_{eff.}(j) = J_A + m_2 \times r^2 \times \sin^2(j);$$

$$C_{eff.}(j, j \otimes j) = m_2 \times r^2 \times \sin(j) \times \cos(j) \times j \otimes r^2;$$

$$Q_{total}(j) = M + F_{r2} \times r \times \sin(j).$$
(22)

Implementation of the Mathematical Model in Wolfram Mathematica Software

The simplified mathematical model derived from the kinetostatic analysis characterizes the in-pipe robot as a hybrid dynamic system. The equations of motion (20), (21), (22) switch depending on the locomotion phase (expansion or contraction), determined by the constraints imposed by the overrunning clutches. A simulation environment was developed using Wolfram Mathematica software to analyze the robot's behavior and validate the model. This section of the paper details the implementation, the numerical methods employed, and the analysis of the simulation results.

The simulation implements the differential equations (20), (21), (22) governing the rotation of the crank (φ) and the resulting translational motion of the modules $(x_1 \text{ and } x_2)$. It is important to note the kinematic convention adopted in the Mathematica implementation. The code determines the relative velocity \mathcal{S} using the expression $-r \times \sin(j)$ $\dot{\mathbf{z}}$. This implies the kinematic transfer function implemented is $K(j) = -r \times \sin(j)$. Consequently, the distance between modules is modeled as $S(j) \times L + r \times \cos(j)$.

The core challenge in simulating this system is handling the discontinuous nature of the dynamics. In the Mathematica code, the switching behavior is implemented using the Piecewise function to define the effective inertia ($J_{eff.}$), the centrifugal terms ($C_{eff.}$), and the generalized forces (Q_{total}).

The simulation utilizes the following input parameters, representing a small-scale in-pipe robot: masses of modules $m_1 = m_2 = 1 \text{ kg}$, crank length (radius) r = 0.05 m, reduced moment of inertia of the crankshaft $J_A = 0.001 \text{ kg} \times \text{m}^2$, resistance (rolling friction) forces $F_{r1} = F_{r2} = 1 \text{ N}$, driving torque (assumed constant) $M = 0.25 \text{ N} \times \text{m}$, connecting rod length L = 0.2 m, and simulation time $T_{sim} = 1 \text{ s}$.

The resulting system of differential equations is stiff and non-smooth due to the Piecewise definitions. To solve this system accurately, the NDSolve function in Mathematica was employed. To ensure stability and accuracy during the abrupt dynamic transitions, the integration method was specified as "StiffnessSwitching". This method is designed to handle hybrid systems efficiently by detecting the state-dependent events (the clutch engagements) and adjusting the integration algorithm to maintain stability and accuracy. High fidelity was ensured by setting AccuracyGoal and PrecisionGoal to 10. The simulation is performed in two stages. First, the dynamic equation for $\varphi(t)$ is solved. Subsequently, the velocities of the modules, $V_1(t)$ and $V_2(t)$, are defined based on the solution $\varphi(t)$ and j & (t), using Piecewise functions to model the clutch engagement. Finally, these velocities are integrated to find the displacements $x_1(t)$ and $x_2(t)$.

The numerical simulation provides insights into the kinematics of the robot during the initial start-up phase under a constant driving torque. Figure 2 illustrates the rotation of the crank $\varphi(t)$. Figure 2a shows the crank angle over the simulation period, measured in revolutions. As the driving torque M (0.25 N·m) is significantly larger than the maximum opposing generalized forces $(F_r \cdot r = 0.05 \text{ N·m})$, the crank continuously accelerates. The non-linear increase in $\varphi(t)$ confirms this acceleration, with the crank completing approximately 8.5 revolutions within the first second. Figure 2b shows the cosine of the crank angle. Since the initial angle $\varphi(0)$ is near zero, the plot starts near 1.0. The increasing frequency of the oscillations visually confirms the acceleration of the crank rotation observed in Fig. 2a.

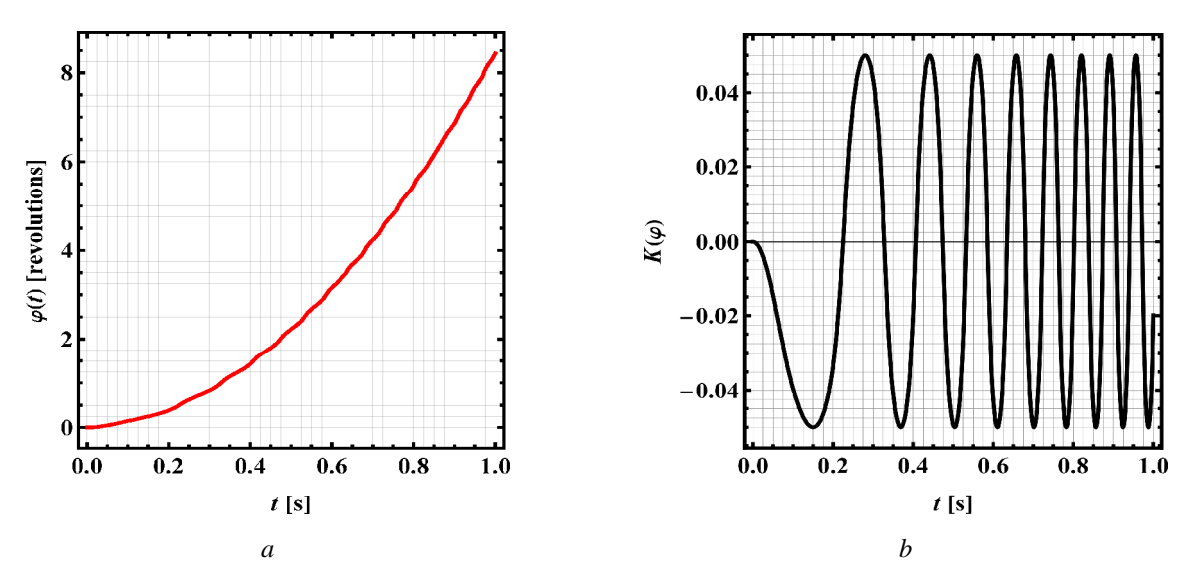


Fig. 2. Time plot of the crank rotation angle (a) and the kinematic transfer function (b) Puc. 2. Часова залежність кута повороту кривошипа (а) та функції кінематичного перетворення (б)

Figure 3a presents the displacements of the rear module $(m_1, black)$ and the front module (m_2, red) . The plots clearly demonstrate the characteristic "inchworm" locomotion pattern. The modules move forward alternately: m_1 moves while m_2 is stationary (contraction), and m_2 moves while m_1 is stationary (expansion). Because the crank rotation speed increases over time (as seen in Fig. 2), the time duration of each step decreases. This results in an overall acceleration of the robot system, reaching a total displacement of approximately 0.9 m for m_1 and 1.0 m for m_2 in 1 second.

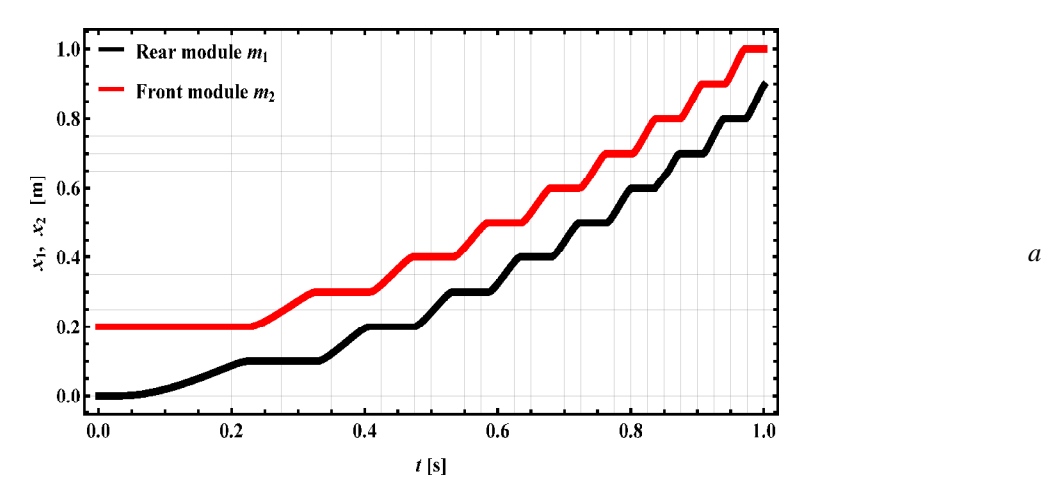


Fig. 3. Simulation results of displacements (a), velocities (b), and accelerations (c) of the robot's modules Puc. 3. Результати моделювання переміщень (a), швидкостей (б) та пришвидшень (в) модулів робота

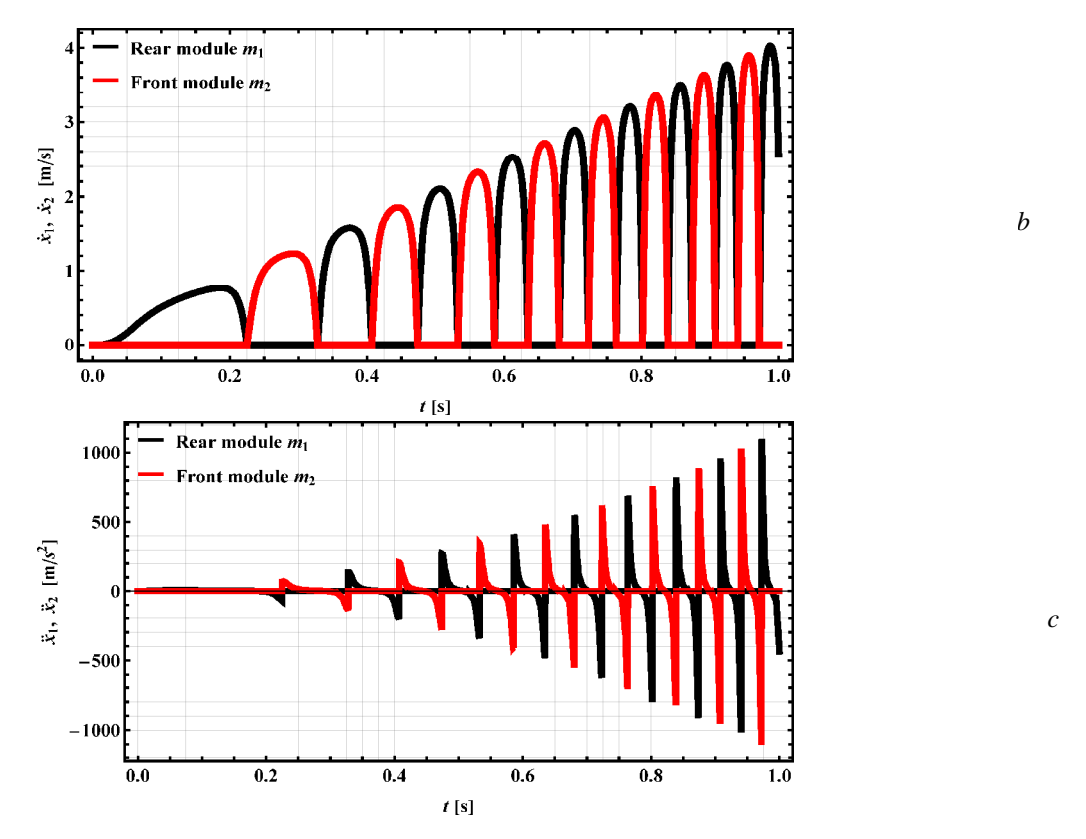


Fig. 3. (Continuation). Simulation results of displacements (a), velocities (b), and accelerations (c) of the robot's modules Рис. 3. (Продовження). Результати моделювання переміщень (а), швидкостей (б) та пришвидшень (в) модулів робота

Figure 3b illustrates the velocities of the two modules. The simulation confirms that the velocities are non-overlapping pulses. When $\Re > 0$, $\Re = 0$, and vice versa. This validates the idealized model of the overrunning clutches, which prevent backward motion. The magnitude of these velocity pulses increases throughout the simulation, reaching nearly 4 m/s by t = 1 s. This increase is directly related to the rising angular velocity of the crank $j\Re(t)$.

The acceleration profiles (Fig. 3c) reveal the dynamic impacts inherent in this type of locomotion system. Extremely large acceleration spikes (both positive and negative) occur at the instants when the locomotion mode switches. These spikes reach magnitudes up to 1000 m/s^2 . This phenomenon is a direct consequence of the simplified model assumptions, specifically the idealization of the clutches as engaging and disengaging instantaneously. The magnitude of these spikes increases as the system velocity increases, highlighting potential practical challenges related to dynamic loads.

To fully understand the locomotion mechanism of the in-pipe robot and validate the mathematical model, it is crucial to analyze the internal motion between the two modules. Figure 4 presents the time history of the relative displacement $(S = x_2 - x_1)$ and the relative velocity $(S = x_2 - x_1)$ during the first second of simulation. The black curve represents the distance between the modules $(x_2 - x_1)$, shown in decimeters [dm] (equivalent to meters \times 10). This distance is determined by the geometry of the internal slider-crank mechanism. Based on the convention adopted in the simulation (where $\varphi = 0$ corresponds to maximum extension), the distance is modeled as $S(j) \times L + r \times cos(j)$.

Using the simulation parameters (L = 0.2 m or 2 dm, and r = 0.05 m or 0.5 dm), the distance is constrained to oscillate between a minimum of $S_{min} = L - r = 1.5$ dm and a maximum of $S_{max} = L + r = 2.5$ dm. The plot accurately reflects this behavior, starting at the maximum extension (2.5 dm) at t = 0. This oscillation represents the periodic extension and contraction of the robot body – the core action of the inchworm drive. The frequency of this oscillation increases visibly over time. This trend is a direct consequence of the accelerating crank rotation (as observed in Fig. 1), driven by the constant input torque.

The red curve in Fig. 4 represents the relative velocity between the modules $(x_2 - x_1)$, shown in [m/s]. This quantity, x_1 , is the time derivative of the relative displacement and is the primary determinant of the robot's locomotion mode. The plot shows that the relative velocity is oscillatory, alternating between positive and negative values:

- 1. Negative relative velocity $(\Re < 0)$. This corresponds to the contraction phase. The distance between the modules is decreasing. In this phase, the front module m_2 is locked $(\Re = 0)$, and the rear module m_1 moves forward $(\Re = -\Re)$.
- 2. Positive Relative Velocity $(\Re > 0)$. This corresponds to the expansion phase. The distance between the modules is increasing. In this phase, the rear module m_1 is locked by its clutch $(\Re = 0)$, and the front module m_2 moves forward $(\Re = \Re)$.

The magnitude of the relative velocity increases significantly during the simulation, starting near 0 m/s and reaching peaks close to $\pm 4 \text{ m/s}$ by t = 1.0 s. This increase is expected because the relative velocity is kinematically related to the crank angular velocity ($\$ = -r \times \sin(j) \times \$$). Since j & is increasing due to the applied torque, the peak relative velocity also increases.

Figure 4 effectively visualizes the internal kinematics and the derivative relationship between the two curves. When the relative displacement (black curve) reaches its maximum value (2.5 dm), the relative velocity (red curve) crosses zero, transitioning from positive to negative. This marks the end of the expansion phase and the beginning of the contraction phase. Conversely, when the relative displacement reaches its minimum value (1.5 dm), the relative velocity crosses zero, transitioning from negative to positive. For example, the first minimum occurs at approximately t = 0.23 s, marking the switch from contraction to expansion. These transition points are critical, as they correspond to the moments when the clutches engage/disengage, causing the switches in the dynamic equations of motion and generating the acceleration spikes previously observed in Fig. 3c.

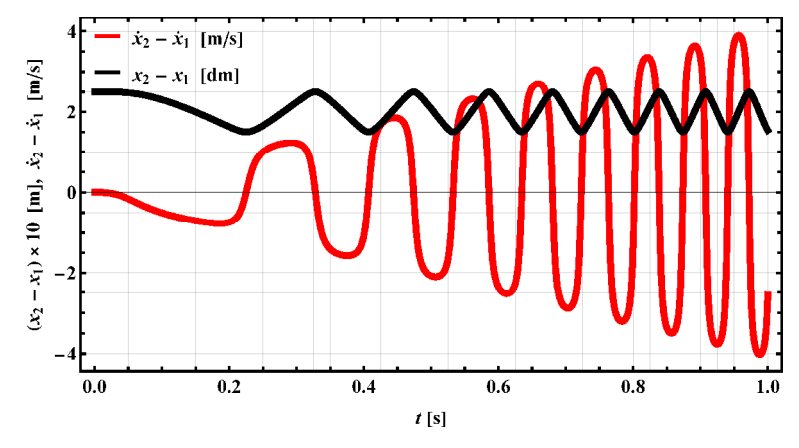


Fig. 4. Time histories of the relative displacement and the relative velocity of the robot's modules Puc. 4. Часові залежності відносного переміщення і відносної швидкості модулів робота

In general, the implementation of the mathematical model in Wolfram Mathematica successfully simulates the hybrid dynamics of the in-pipe robot. The use of the "StiffnessSwitching" method allowed for an accurate solution, confirming the viability of the inchworm locomotion strategy and providing valuable insights into the system's dynamic behavior.

Conclusions

This paper presented a comprehensive kinetostatic analysis of the propulsion system for a mobile in-pipe inspection robot utilizing an inchworm locomotion strategy. The study addressed the identified gap in the literature regarding the lack of unified analytical frameworks that connect the kinematics of motion with the required forces for complex IPIRs. The main conclusions of this research are summarized as follows.

A simplified mathematical model for the two-module in-pipe robot, equipped with an internal slider-crank mechanism and overrunning clutches, was successfully derived using the Lagrangian approach. This model accurately captures the hybrid dynamic nature of the system, defining the distinct equations of motion, effective inertia, and generalized forces for the expansion and contraction phases based on the generalized coordinate of the crank rotation.

The implementation of the model in Wolfram Mathematica, utilizing the "StiffnessSwitching" numerical integration method, effectively handled the stiff and non-smooth differential equations. The simulations confirmed the viability of the inchworm locomotion strategy, clearly demonstrating the alternating movement of the modules and the rectification of internal oscillations into net forward propulsion.

The simulation provided valuable insights into the robot's start-up dynamics under a constant driving torque. The results showed that the robot continuously accelerates as the crank rotation speed increases. The velocity analysis validated the function of the idealized overrunning clutches, showing non-overlapping velocity pulses that increase in magnitude with time.

A critical finding of the kinetostatic analysis is the presence of significant dynamic impacts, characterized by extremely large acceleration spikes (up to 1000 m/s²) at the instants when the locomotion mode switches. This phenomenon is attributed to the assumption of instantaneous clutch engagement and highlights a crucial area for practical design considerations, suggesting the need for incorporating compliance or more sophisticated clutch models in future work.

In general, the developed kinetostatic framework provides a robust analytical foundation for the design optimization and control of inchworm-type in-pipe robots, advancing the capabilities of robotic systems for pipeline integrity management.

References

- 1. Elankavi, R. S. et al. A review on wheeled type in-pipe inspection robot // International Journal of Mechanical Engineering and Robotics Research. 2022. Vol. 11, No. 10. P. 745–754. https://doi.org/10.18178/ijmerr.11.10.745-754
- 2. John, B., Shafeek, M. Pipe inspection robots: a review // IOP Conference Series: Materials Science and Engineering. 2022. Vol. 1272, No. 1. P. 012016. https://doi.org/10.1088/1757-899x/1272/1/012016
- 3. Bekhit, A., Dehghani, A., Richardson, R. Kinematic analysis and locomotion strategy of a pipe inspection robot concept for operation in active pipelines // International Journal of Mechanical Engineering and Mechatronics. 2012. Vol. 1, No. 1. P. 15–27. https://doi.org/10.11159/ijmem.2012.003
- 4. Kahnamouei, J. T., Moallem, M. A comprehensive review of in-pipe robots // Ocean Engineering. 2023. Vol. 277. P. 114260. https://doi.org/10.1016/j.oceaneng.2023.114260
- 5. Elankavi, R. S. Developments in inpipe inspection robot: A review // Journal of Mechanics of Continua and Mathematical Sciences. 2020. Vol. 15, No. 5. P. 238–248. https://doi.org/10.26782/jmcms.2020.05.00022
- 6. Rusu, C., Tatar, M. O. Adapting mechanisms for in-pipe inspection robots: a review // Applied Sciences. 2022. Vol. 12, No. 12. P. 6191. https://doi.org/10.3390/app12126191
- 7. Han, M., et al. Analysis of in-pipe inspection robot structure design // Proceedings of the 2016 2nd Workshop on Advanced Research and Technology in Industry Applications. Paris, France: Atlantis Press, 2016. P. 989–993. https://doi.org/10.2991/wartia-16.2016.210

- 8. Blewitt, G., et al. A review of worm-like pipe inspection robots: research, trends and challenges // Soft Science. 2024. Vol. 4, No. 2. P. 13. https://doi.org/10.20517/ss.2023.49
- 9. Elankavi, R. S., et al. Kinematic modeling and analysis of wheeled in-pipe inspection mobile robot // Handbook of Smart Materials, Technologies, and Devices / ed. Hussain C.M., Di Sia P. Cham: Springer International Publishing, 2021. P. 1–15. https://doi.org/10.1007/978-3-030-58675-1_168-1
- 10. Song, Z., et al. Kinematic analysis and motion control of wheeled mobile robots in cylindrical workspaces // IEEE Transactions on Automation Science and Engineering. 2016. Vol. 13, No. 2. P. 1207–1214. https://doi.org/10.1109/ TASE.2015.2503283
- 11. Castillo-Castañeda, E., Córdoba-Malaver, A. R. Mobile robot with wheeled-legs for inspection of pipes with variable diameter and elbow shapes // Mechanisms and Machine Science. 2021. Vol. 93. P. 325–331. https://doi.org/10.1007/978-3-030-58104-6_37
- 12. Li, P., et al. Design and analysis of a novel active screw-drive pipe robot // Advances in Mechanical Engineering, 2018. Vol. 10, No. 10. P. 1–18. https://doi.org/10.1177/1687814018801384
- 13. Tourajizadeh, H., Afshari, S., Azimi, M. Design and modeling of an in-pipe inspection robot with repairing capability equipped with a manipulator // AUT Journal of Modeling and Simulation. 2021. Vol. 53, No. 1. P. 39–48. https://doi.org/10.22060/miscj.2021.19033.5229
- 14. Zhao, Y., Hua, Y., Di, J. Kinematics modeling and simulation analysis of wheeled mobile robot in round pipe // Proceedings of the 2016 4th International Conference on Sensors, Mechatronics and Automation (ICSMA 2016). Paris, France: Atlantis Press, 2016. Vol. 136. P. 544–550. https://doi.org/10.2991/icsma-16.2016.95
- 15. Zhao, W., Zhang, L., Kim, J. Design and analysis of independently adjustable large in-pipe robot for long-distance pipeline // Applied Sciences. 2020. Vol. 10, No. 10. P. 3637. https://doi.org/10.3390/app10103637
- 16. Lock, J., Dupont, P. E. Friction modeling in concentric tube robots // 2011 IEEE International Conference on Robotics and Automation. 2011. Vol. 23, No. 1. P. 1139–1146. https://doi.org/10.1109/ICRA.2011.5980347
- 17. Korendiy, V. Generalized design diagram and mathematical model of suspension system of vibration-driven robot // Ukrainian Journal of Mechanical Engineering and Materials Science. 2021. Vol. 7, № 3–4. P. 1–10. https://doi.org/10.23939/ujmems2021.03-04.001
- 18. Korendiy V., et al. Mathematical modeling and computer simulation of the wheeled vibration-driven inpipe robot motion // Vibroengineering Procedia. 2022. Vol. 44. P. 1–7. https://doi.org/10.21595/vp.2022.22832
- 19. Korendiy, V., et al. Development and investigation of the vibration-driven in-pipe robot // Vibroengineering Procedia. 2023. Vol. 50. P. 1–7. https://doi.org/10.21595/vp.2023.23513
- 20. Korendiy, V., Kachur, O. Locomotion characteristics of a wheeled vibration-driven robot with an enhanced pantograph-type suspension // Frontiers in Robotics and AI. 2023. Vol. 10. P. 1239137. https://doi.org/10. 3389/frobt.2023.1239137

В. М. Корендій, О. М. Янів, Т. Р. Вільчинський, В. М. Пігарев

Національний університет "Львівська політехніка"

КІНЕТОСТАТИЧНИЙ АНАЛІЗ ПРИВІДНОГО МЕХАНІЗМУ МОБІЛЬНОГО РОБОТА ДЛЯ МОНІТОРИНГУ ВНУТРІШНІХ ПОВЕРХОНЬ ТРУБОПРОВОДІВ

Постановка проблеми. Структурна цілісність розгалужених трубопровідних мереж є критично важливою для економічної та екологічної безпеки, що потребує надійних методів моніторингу їхнього стану. Мобільні роботи для внутрішньотрубного інспектування (РВТІ) є одним з ефективних рішень, які не потребують зупинки експлуатації трубопроводу, однак проєктування їхніх привідних механізмів для роботи в обмежених і складних середовищах залишається складним завданням. Наявні аналітичні підходи часто демонструють розрив між кінематичним моделюванням (плануванням руху) та силовим аналізом (стійкість і тягові характеристики), особливо для передових гібридних стратегій переміщення. Ця прогалина перешкоджає систематичній оптимізації та ефективному керуванню конструкціями РВТІ. Мета дослідження. Це дослідження спрямоване на розробку та аналіз комплексної кінетостатичної моделі привідного механізму специфічної конструкції РВТІ: двомодульного робота, що використовує крокуючий (черв'якоподібний) принцип переміщення, приводиться в рух внутрішнім

кривошипно-повзунним механізмом та оснащений обгінними муфтами (муфтами вільного ходу). Метою є створення математичної моделі, яка точно пов'язує кінематику руху з силами, необхідними для його здійснення. Методологія. У дослідженні застосовується кінетостатичний аналіз на основі рівнянь Лагранжа. Робот розглядається як гібридна динамічна система, що функціонує у двох різних режимах: розширення та стиснення. Кут повороту кривошипа прийнято за узагальнену координату. Рівняння руху виведені для кожного режиму з урахуванням обмежень, що накладаються ідеальними обгінними муфтами, які забезпечують однонапрямлений рух. Отримані жорсткі та негладкі диференціальні рівняння реалізовано у програмному середовищі Wolfram Mathematica та розв'язано чисельно з використанням методу "StiffnessSwitching" для точного опрацювання розривної динаміки. Результати. Чисельне моделювання успішно підтверджує крокуючий принцип переміщення, демонструючи характерний почерговий рух модулів. За умови постійного рушійного моменту (0.25 Нм), робот демонструє неперервне пришвидшення, досягаючи пікових швидкостей приблизно 4 м/с протягом першої секунди. Аналіз профілів швидкостей підтверджує брак перекриття руху модулів, що валідує ідеалізовану модель муфт. Ключовим висновком є наявність надзвичайно великих піків прискорення (до 1000 м/с²), що виникають миттєво під час переходу між режимами руху. Це вказує на значні динамічні удари, властиві цій стратегії переміщення. Наукова новизна. Новизна полягає у строгому виведенні кінетостатичної моделі, спеціально адаптованої для крокуючого РВТІ з обгінними муфтами. Застосування механіки Лагранжа до цієї гібридної динамічної системи забезпечує уніфіковану аналітичну основу, яка долає розрив між генеруванням руху та аналізом сил для цього класу роботів. Практична цінність. Розроблена математична модель є потужним інструментом для оптимізації конструктивних параметрів (наприклад, розподілу мас, геометрії механізму, вибору приводів) крокуючих РВТІ. Вона дає критичне розуміння динамічної поведінки системи, зокрема наголошує на неодмінності зменшення високих динамічних навантажень, що виникають під час вмикання муфт у практичних реалізаціях. Напрямки подальших досліджень. Подальші дослідження повинні бути зосереджені на вдосконаленні математичної моделі для врахування неідеальної поведінки муфт (наприклад, податливості та динаміки тертя), аналізі переміщення у складних геометріях (вигини й вертикальні ділянки) та розробці стратегій керування на основі запропонованої динамічної моделі.

Ключові слова: робот для внутрішньотрубного інспектування, кінетостатичний аналіз, крокуючий принцип переміщення, гібридна динамічна система, механіка Лагранжа, обгінна муфта, кривошипно-повзунний механізм, математичне моделювання, чисельне моделювання.

Інформаційні джерела

- 1. Elankavi R. S. et al. A review on wheeled type in-pipe inspection robot // International Journal of Mechanical Engineering and Robotics Research. 2022. Vol. 11, No. 10. P. 745–754. https://doi.org/10.18178/ijmerr.11.10.745-754
- 2. John B., Shafeek M. Pipe inspection robots: a review // IOP Conference Series: Materials Science and Engineering. 2022. Vol. 1272, No. 1. P. 012016. https://doi.org/10.1088/1757-899x/1272/1/012016
- 3. Bekhit A., Dehghani A., Richardson R. Kinematic analysis and locomotion strategy of a pipe inspection robot concept for operation in active pipelines // International Journal of Mechanical Engineering and Mechatronics. 2012. Vol. 1, No. 1. P. 15–27. https://doi.org/10.11159/ijmem.2012.003
- 4. Kahnamouei J.T., Moallem M. A comprehensive review of in-pipe robots // Ocean Engineering. 2023. Vol. 277. P. 114260. https://doi.org/10.1016/j.oceaneng.2023.114260
- 5. Elankavi R.S. Developments in inpipe inspection robot: A review // Journal of Mechanics of Continua and Mathematical Sciences. 2020. Vol. 15, No. 5. P. 238–248. https://doi.org/10.26782/jmcms.2020.05.00022
- 6. Rusu C., Tatar M.O. Adapting mechanisms for in-pipe inspection robots: a review // Applied Sciences. 2022. Vol. 12, No. 12. P. 6191. https://doi.org/10.3390/app12126191
- 7. Han M. et al. Analysis of in-pipe inspection robot structure design // Proceedings of the 2016 2nd Workshop on Advanced Research and Technology in Industry Applications. Paris, France: Atlantis Press, 2016. P. 989–993. https://doi.org/10.2991/wartia-16.2016.210
- 8. Blewitt G. et al. A review of worm-like pipe inspection robots: research, trends and challenges // Soft Science. 2024. Vol. 4, No. 2. P. 13. https://doi.org/10.20517/ss.2023.49
- 9. Elankavi R.S. et al. Kinematic modeling and analysis of wheeled in-pipe inspection mobile robot // Handbook of Smart Materials, Technologies, and Devices / ed. Hussain C.M., Di Sia P. Cham: Springer International Publishing, 2021. P. 1–15. https://doi.org/10.1007/978-3-030-58675-1_168-1

- 10. Song Z. et al. Kinematic analysis and motion control of wheeled mobile robots in cylindrical workspaces // IEEE Transactions on Automation Science and Engineering. 2016. Vol. 13, No. 2. P. 1207–1214. https://doi.org/10. 1109/TASE.2015.2503283
- 11. Castillo-Castañeda E., Córdoba-Malaver A.R. Mobile robot with wheeled-legs for inspection of pipes with variable diameter and elbow shapes // Mechanisms and Machine Science. 2021. Vol. 93. P. 325–331. https://doi.org/10.1007/978-3-030-58104-6 37
- 12. Li P. et al. Design and analysis of a novel active screw-drive pipe robot // Advances in Mechanical Engineering. 2018. Vol. 10, No. 10. P. 1–18. https://doi.org/10.1177/1687814018801384
- 13. Tourajizadeh H., Afshari S., Azimi M. Design and modeling of an in-pipe inspection robot with repairing capability equipped with a manipulator // AUT Journal of Modeling and Simulation. 2021. Vol. 53, No. 1. P. 39–48. https://doi.org/10.22060/miscj.2021.19033.5229
- 14. Zhao Y., Hua Y., Di J. Kinematics modeling and simulation analysis of wheeled mobile robot in round pipe // Proceedings of the 2016 4th International Conference on Sensors, Mechatronics and Automation (ICSMA 2016). Paris, France: Atlantis Press, 2016. Vol. 136. P. 544–550. https://doi.org/10.2991/icsma-16.2016.95
- 15. Zhao W., Zhang L., Kim J. Design and analysis of independently adjustable large in-pipe robot for long-distance pipeline // Applied Sciences. 2020. Vol. 10, No. 10. P. 3637. https://doi.org/10.3390/app10103637
- 16. Lock J., Dupont P.E. Friction modeling in concentric tube robots // 2011 IEEE International Conference on Robotics and Automation. 2011. Vol. 23, No. 1. P. 1139–1146. https://doi.org/10.1109/ICRA.2011.5980347
- 17. Korendiy V. Generalized design diagram and mathematical model of suspension system of vibration-driven robot // Ukrainian Journal of Mechanical Engineering and Materials Science. 2021. Vol. 7, № 3–4. P. 1–10. https://doi.org/10.23939/ujmems2021.03-04.001
- 18. Korendiy V. et al. Mathematical modeling and computer simulation of the wheeled vibration-driven inpipe robot motion // Vibroengineering Procedia. 2022. Vol. 44. P. 1–7. https://doi.org/10.21595/vp.2022.22832
- 19. Korendiy V. et al. Development and investigation of the vibration-driven in-pipe robot // Vibroengineering Procedia. 2023. Vol. 50. P. 1–7. https://doi.org/10.21595/vp.2023.23513
- 20. Korendiy V., Kachur O. Locomotion characteristics of a wheeled vibration-driven robot with an enhanced pantograph-type suspension // Frontiers in Robotics and AI. 2023. Vol. 10. P. 1239137. https://doi.org/10.3389/frobt.2023.1239137